Vibration isolation in KAGRA

Ryutaro Takahashi
(National Astronomical Observatory of Japan)
and
KAGRA collaboration

GWADW2019
Hotel Hermitage, Isola d'Elba, 19-25 May 2019

Outline

1. Configuration & Installation
2. Control
    1. Filter chain
    2. Inverted Pendulum
3. Evaluation

1. Configuration and installation

Configuration of vibration isolation system

Type-A: for cryogenic mirrors
Type-B: for room temperature mirrors
Type-Bp: simpler Type-B
Type-C: for small optics

Type-A

Type-B

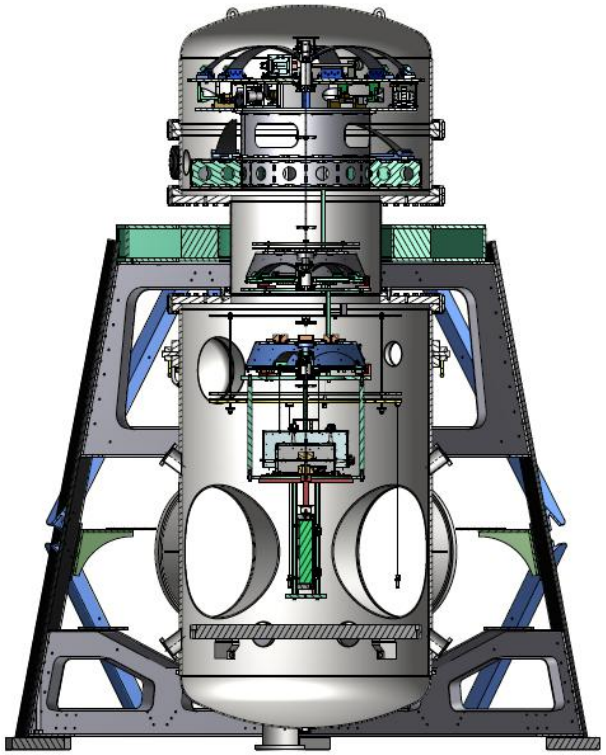

Type-Bp

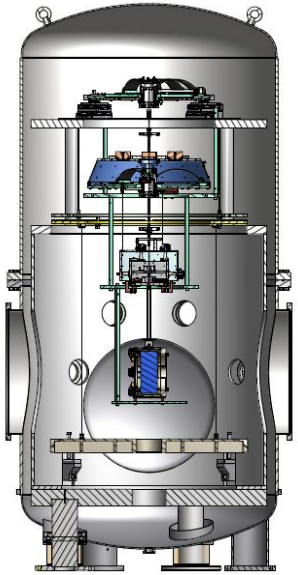

Type-C

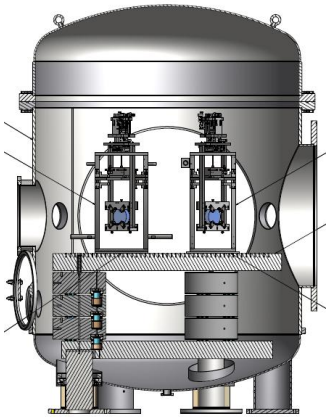

Seismic Attenuation System (Type-B)

Pre-isolator (PI)
- Top Filter (TF)
- Inverted Pendulum (IP)

Filter chain
- Standard Filter (SF)
  Filter1~3 in Type-A
  Filter1 in Type-B
- Bottom Filter (BF)

Payload (PAY)
- Intermediate Mass (IM)
  Intermediate Recoil Mass (IRM)
- Test Mass (TM)
  Recoil Mass (RM)

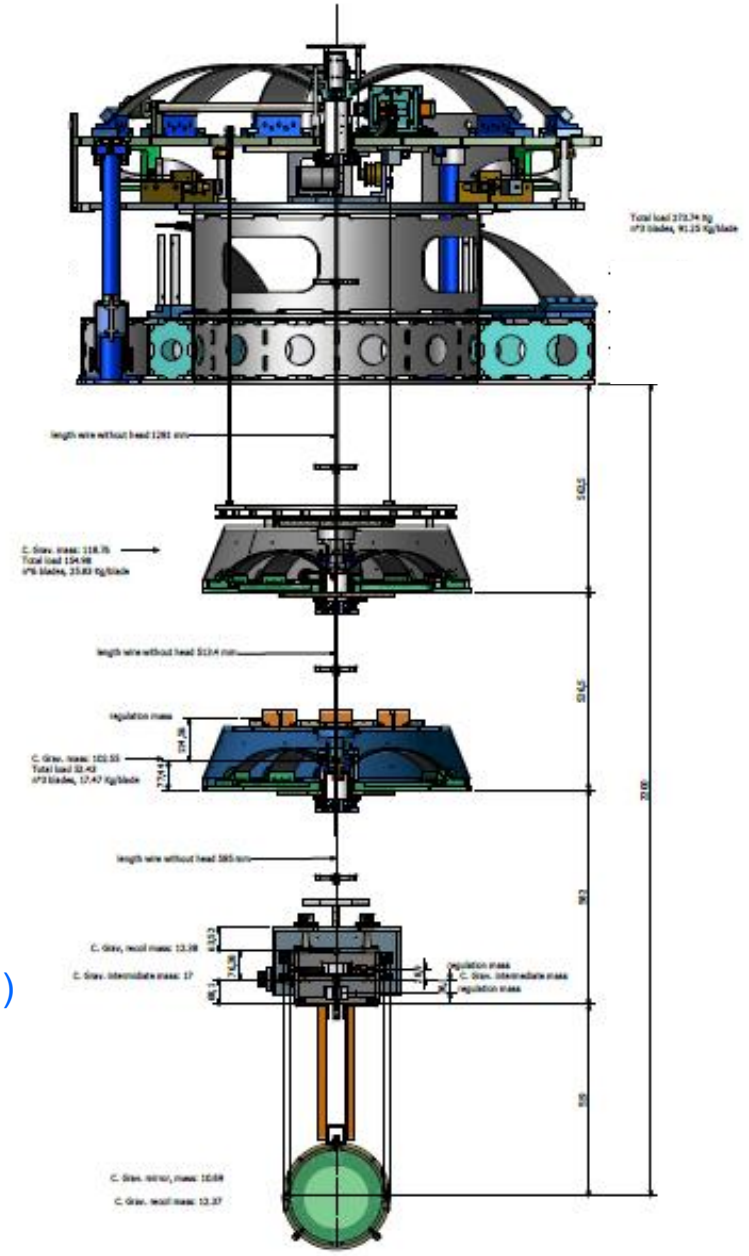

Type-A Tower

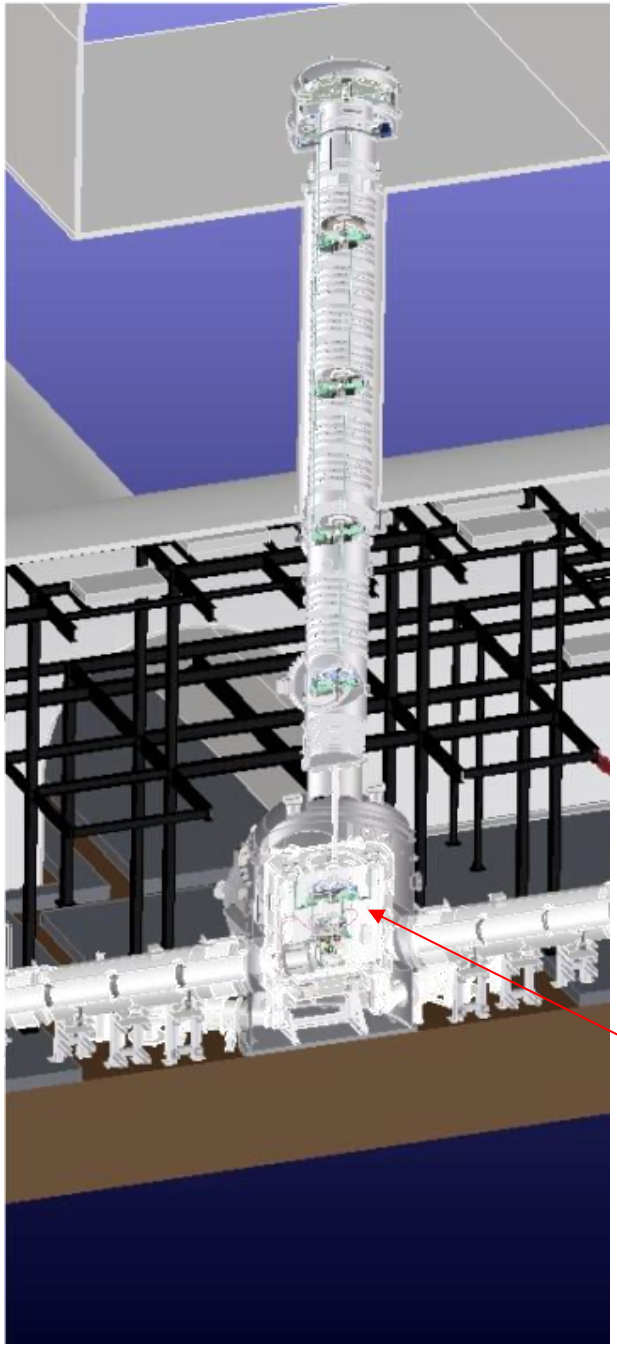
2nd Floor
Bore Hole
1st Floor
Cryo-payload


Pre-isolator
(IP+F0)
Filter1 (F1)
Filter2 (F2)
Filter3 (F3)
Bottom Filter (BF)
10m

Installation

iKAGRA

bKAGRA phase 1

bKAGRA phase 2

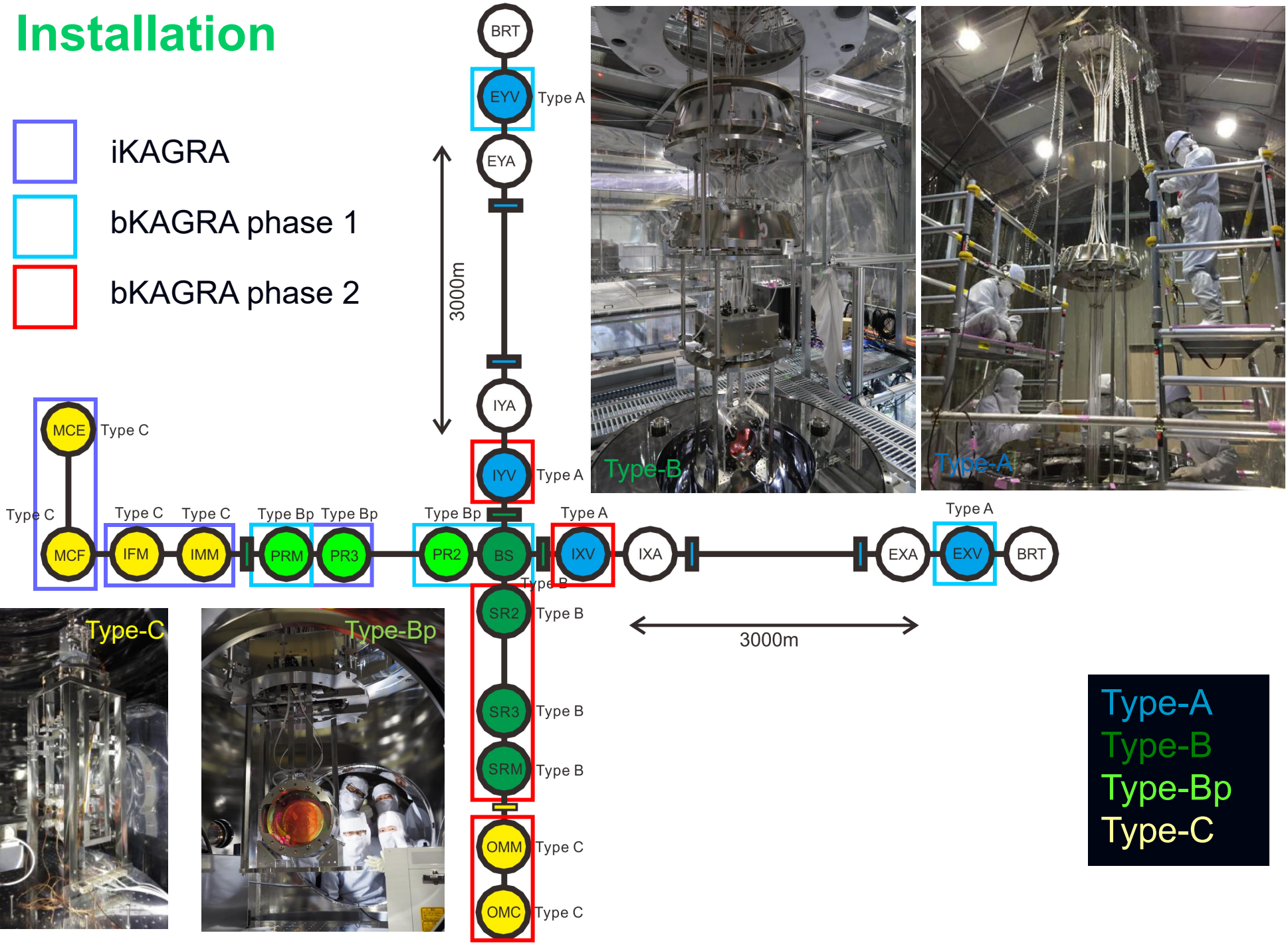

2. Control

Control scheme

IP servo (3 DOF)
- 3 horizontal LVDT-Actuator units
- 3 horizontal inertial sensors

GAS servo (1 DOF)
- 1 vertical LVDT-Actuator unit

BF servo (6 DOF)
- 3 horizontal LVDT-Actuator units
- 3 vertical LVDT-Actuator units

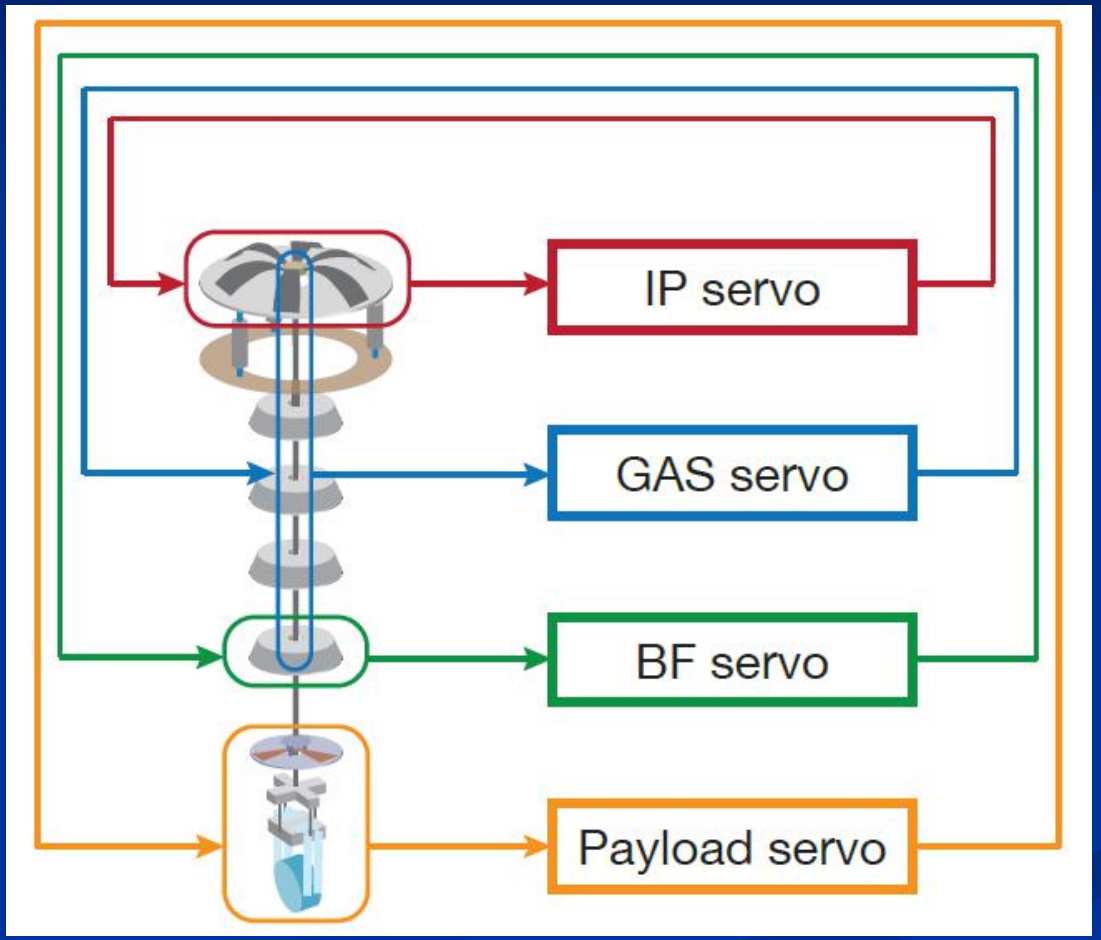

2-1. Control of filter chain

Transfer functions of GAS filter

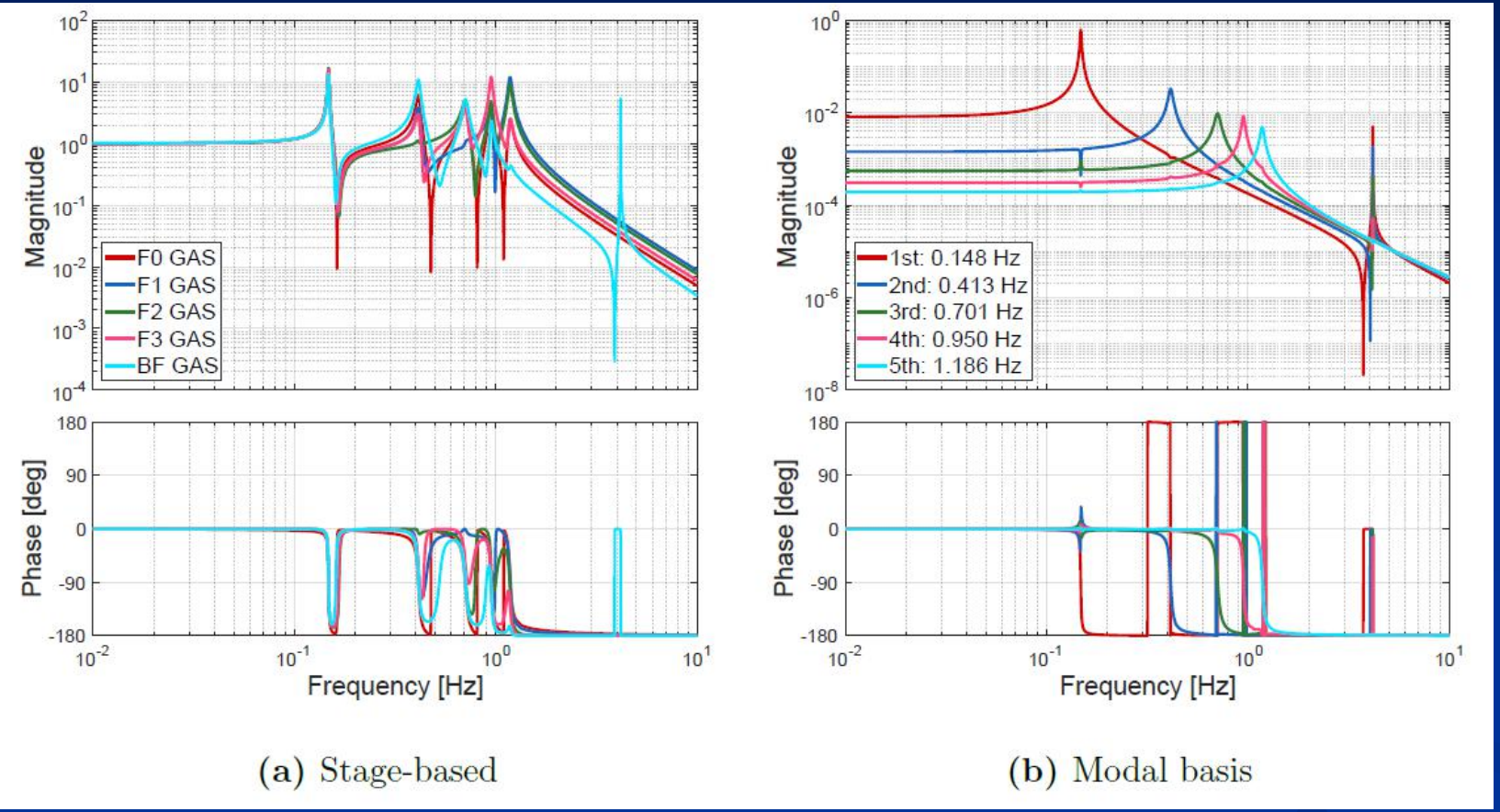

by K. Okutomi

Calculated transfer functions of the GAS filter stage in vertical direction.
(a) Stage based: Response from Actuator to LVDT in each stage.
(b) Modal basis: Decomposed single modes

Filter design of damping control

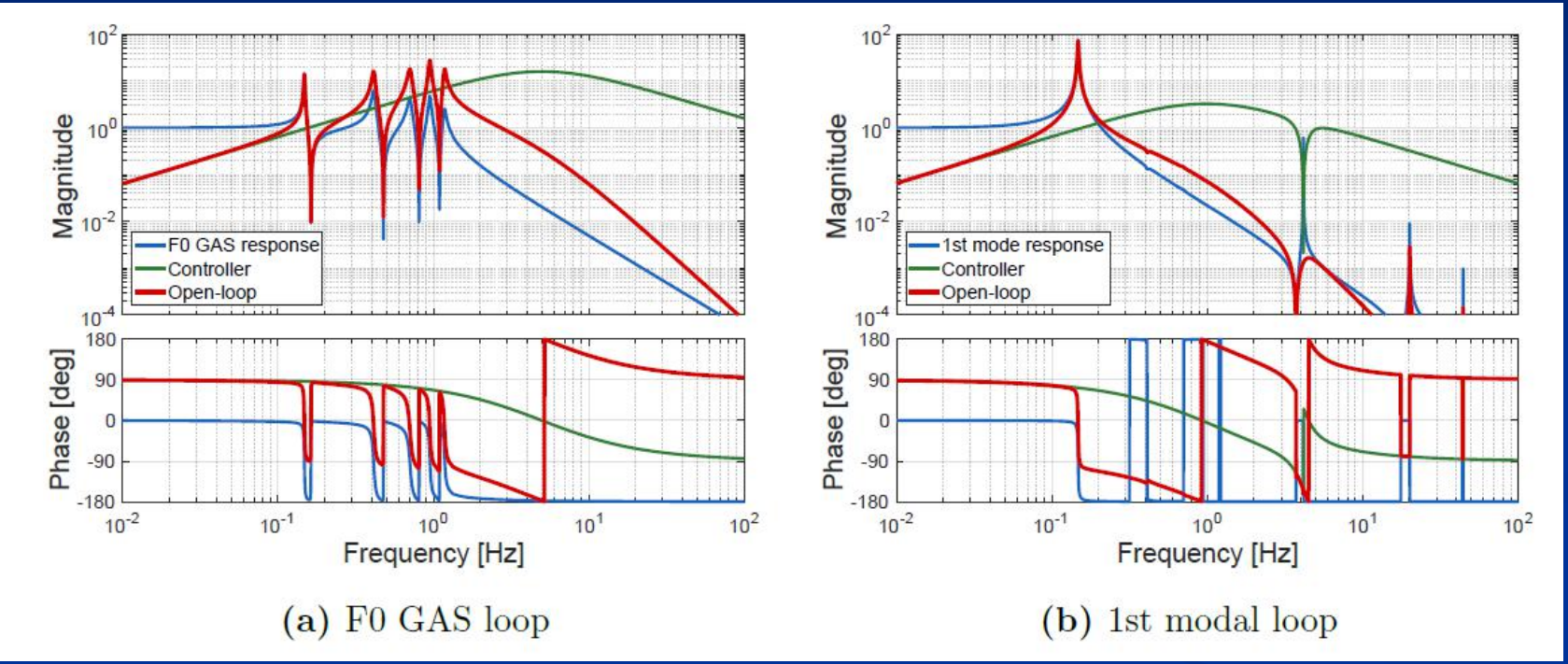

by K. Okutomi

Example of filter design in the stage based (a) and modal basis (b).

Evaluation by decay time

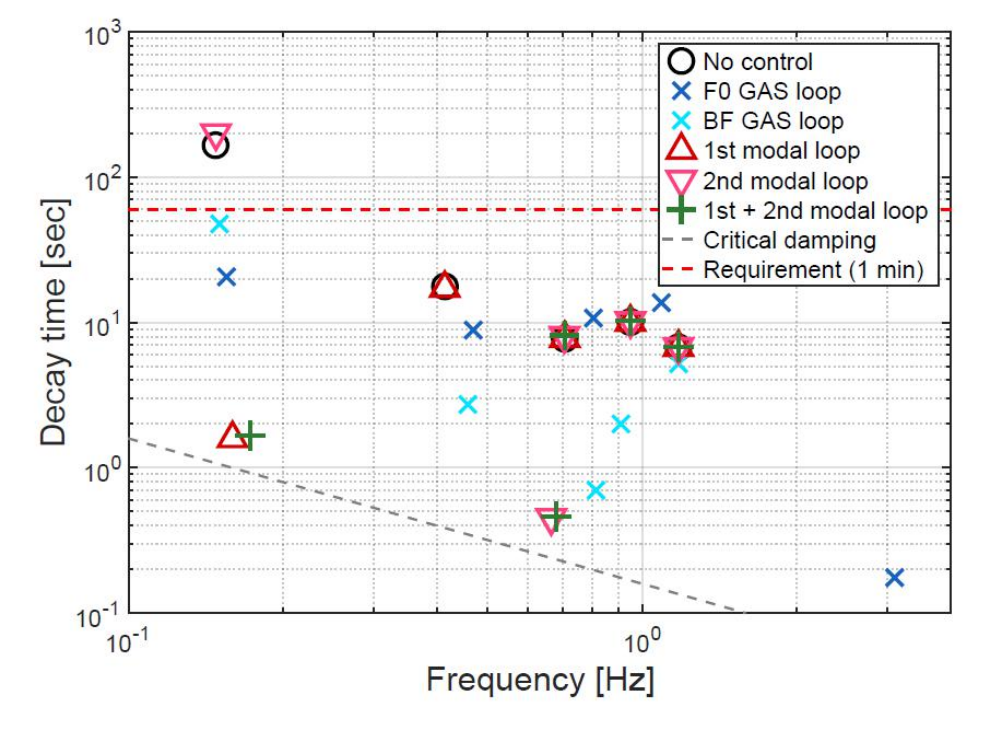

Simulated exponention decay time reduction with various damping controls.

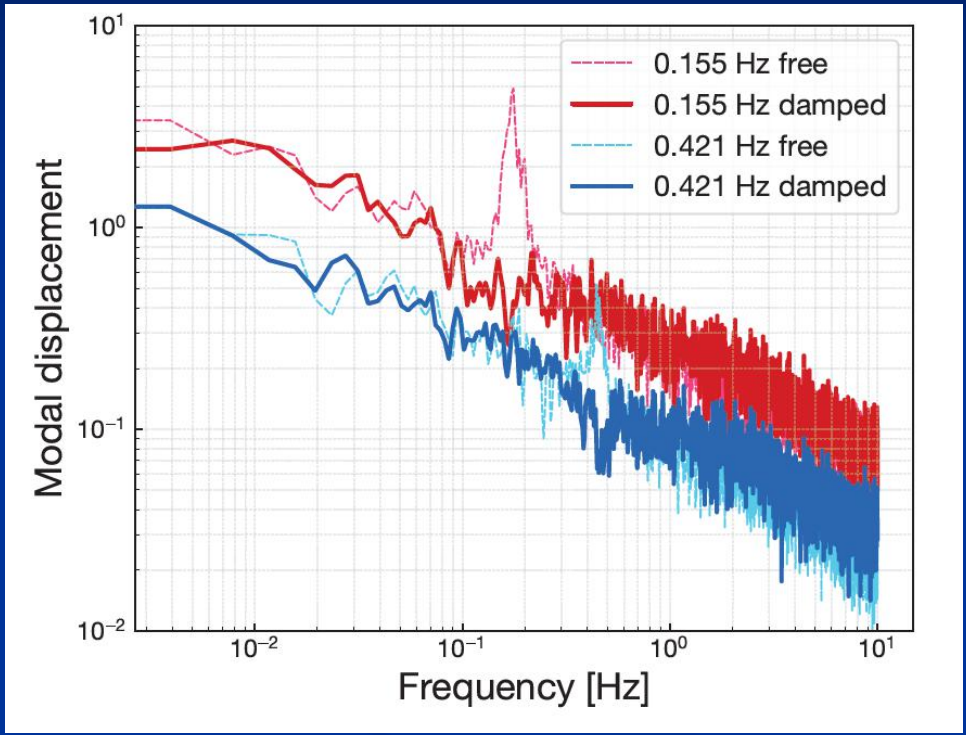

by K. Okutomi

Results of damping control in the modal coordinate.

3-2. Control of Inverted Pendulum

IP control and inertial damping

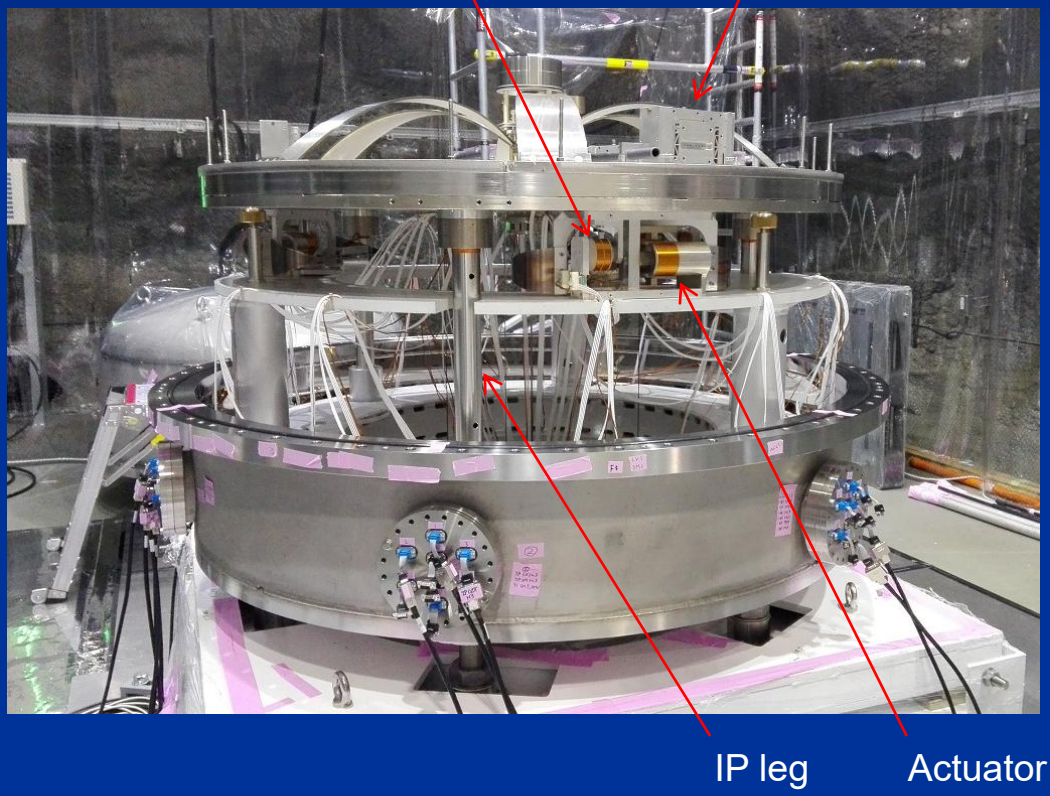

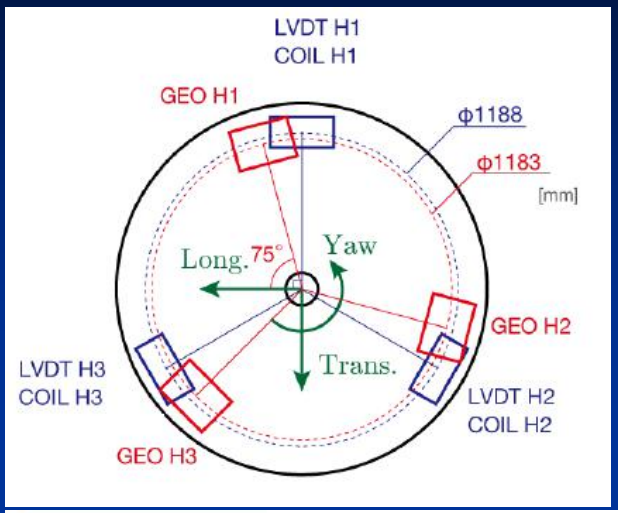

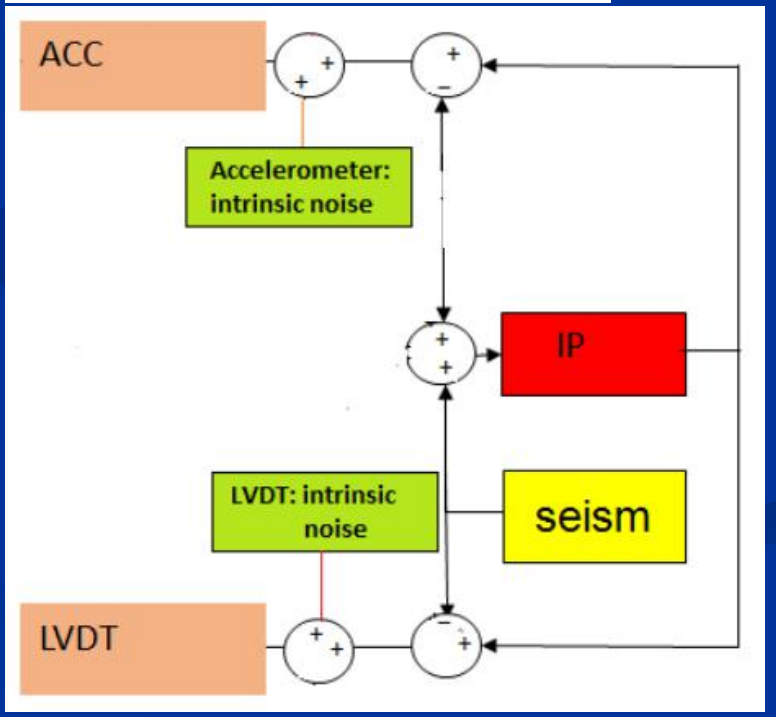

Blending filters for seismic noise reduction

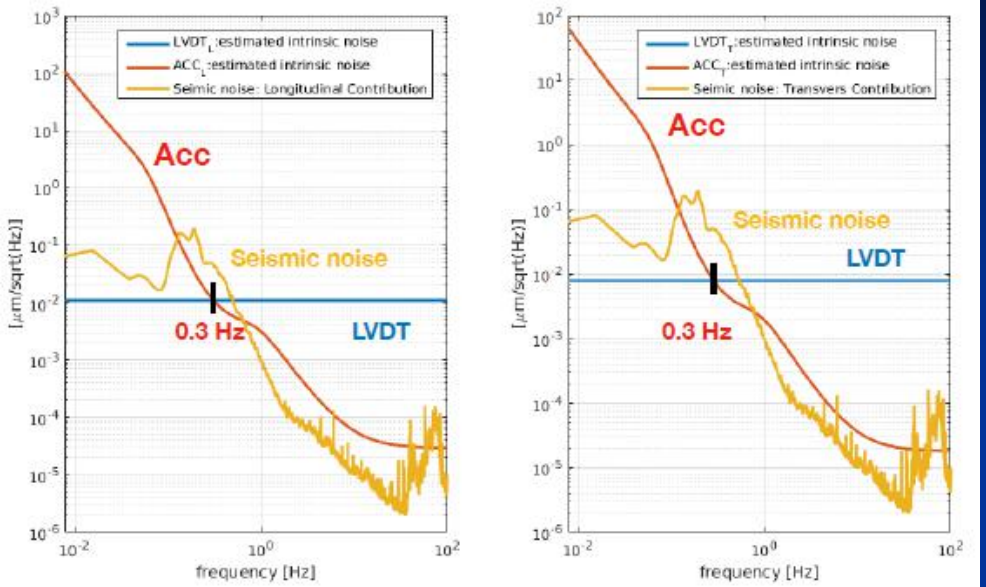

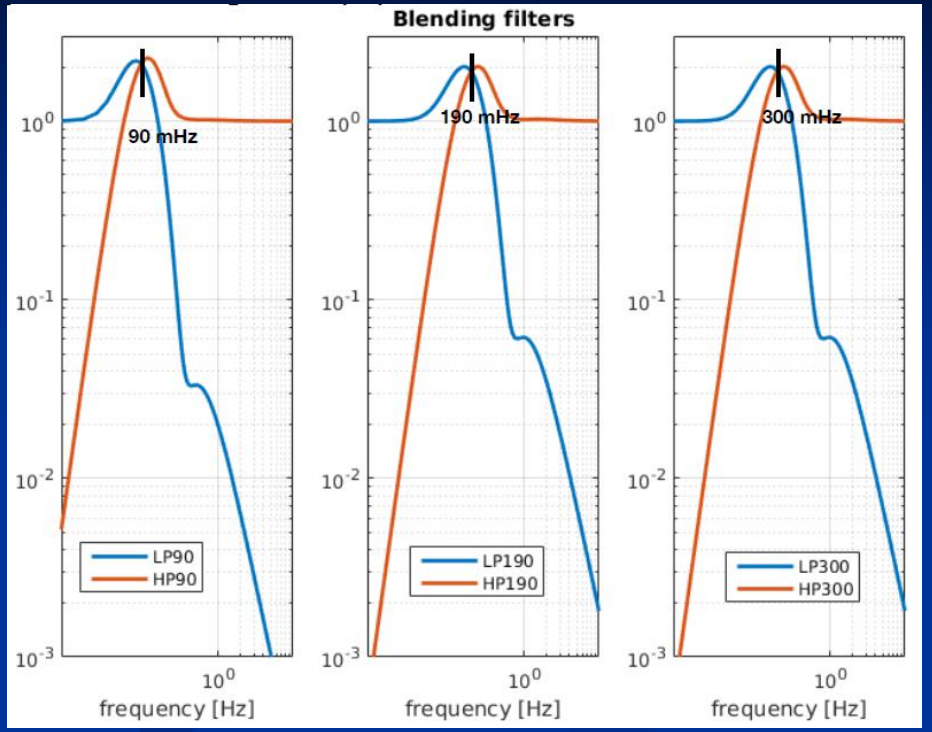

by L. Trozzo

Blending point of LVDT loop (LP) and ACC/Geopone loop (HP) depends on the sensor noise. The 90 mHz is shaped to reduce the re-injection of seismic noise in the range of 0.2-0.5 Hz

Residual motion of IP

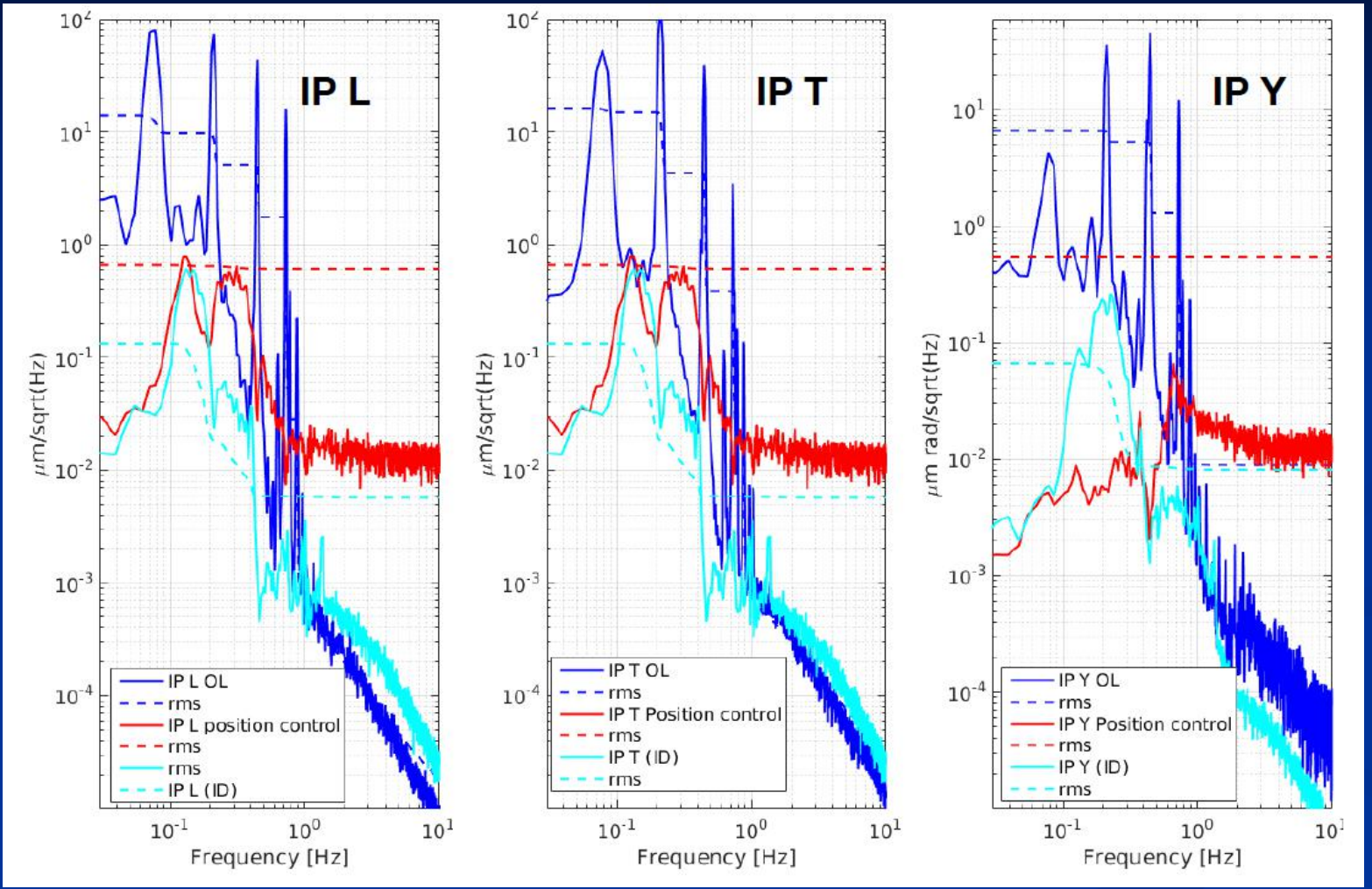

by L. Trozzo

Results of inertial damping in ITMX. ACCs are used as inertial sensor. The blending frequency was 190mHz for L and T, and 300mHz for Yaw respectivery.

Poster #83: L. Trozzo, Preliminary performance of KAGRA's Type A suspension control

3. Evaluation

Setup

Geophone pod

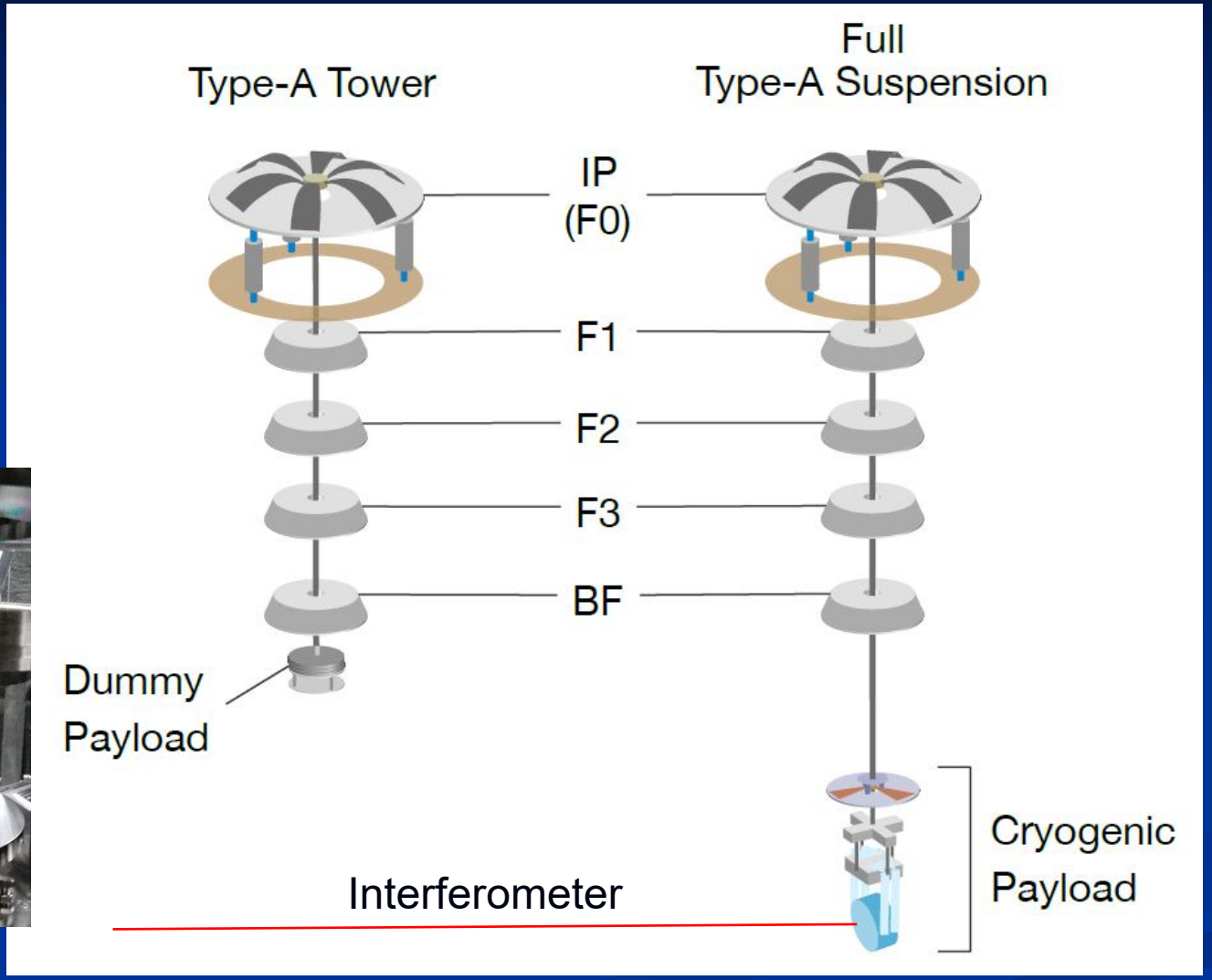

To evaluate the Type-A tower, the dummy payload with geophones (horizontal and vertical) was used as well as the interferometer.

Vibration isolation ratio

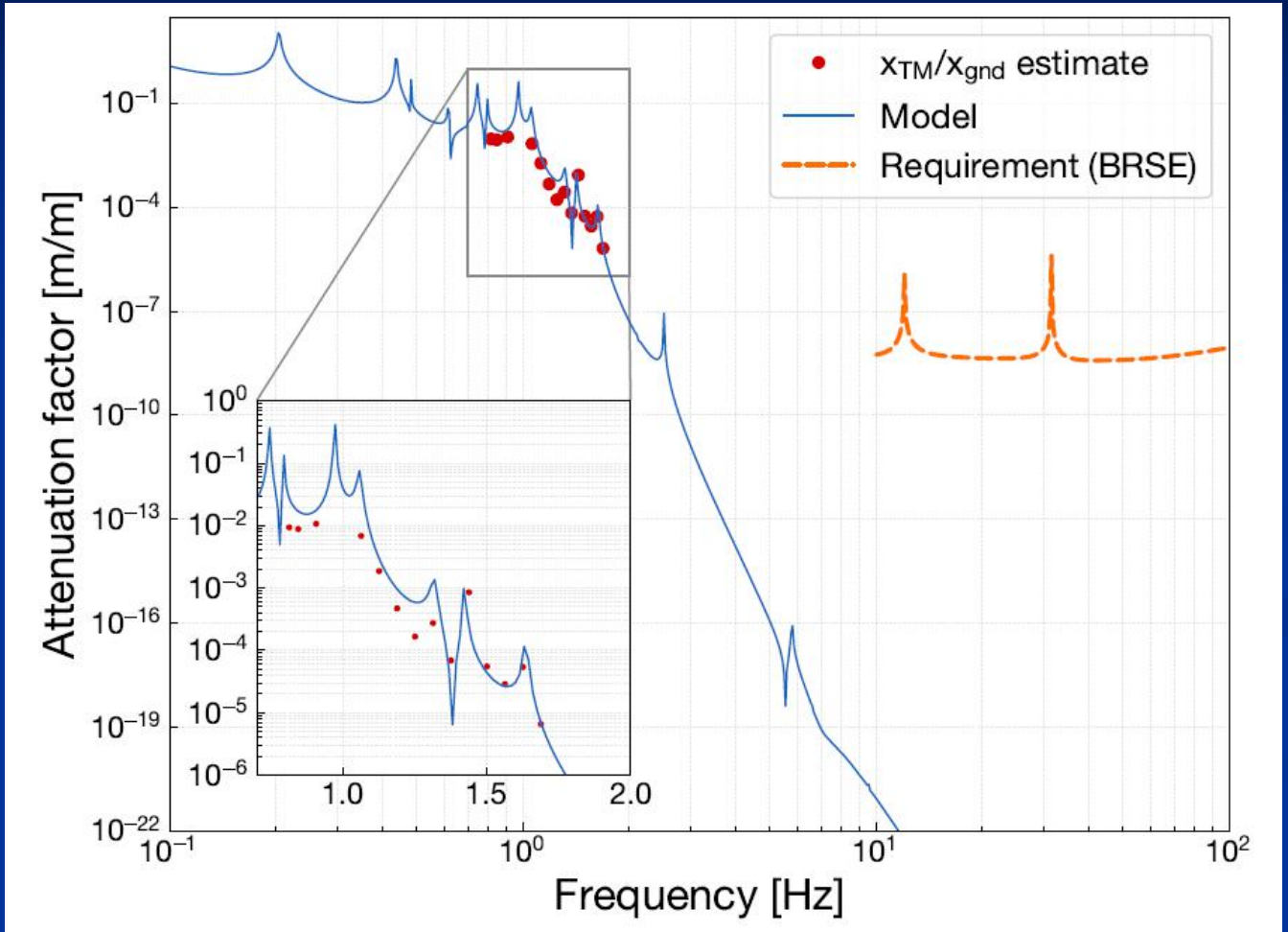

by K. Okutomi

Estimated vibration isolation ratio from the transfer function measured by the 3-km Michelson interferometer in bKAGRA phase-1.

Displacement of IP

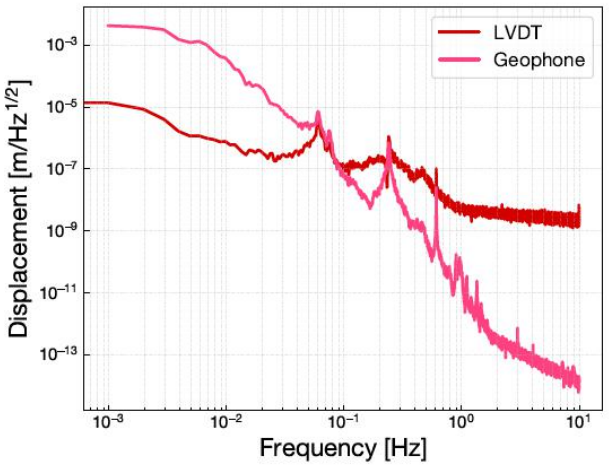

(a) Longitudinal

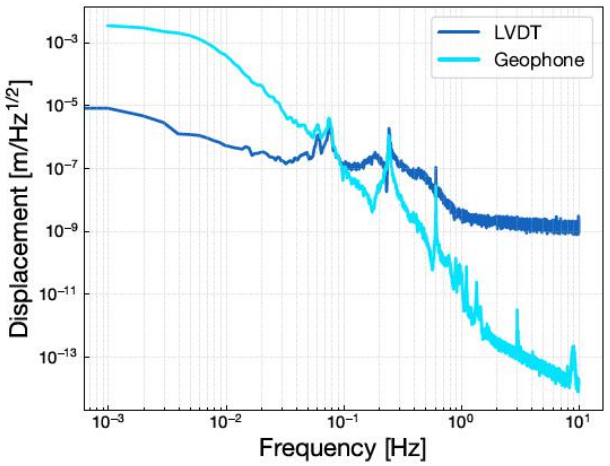

(b) Transverse

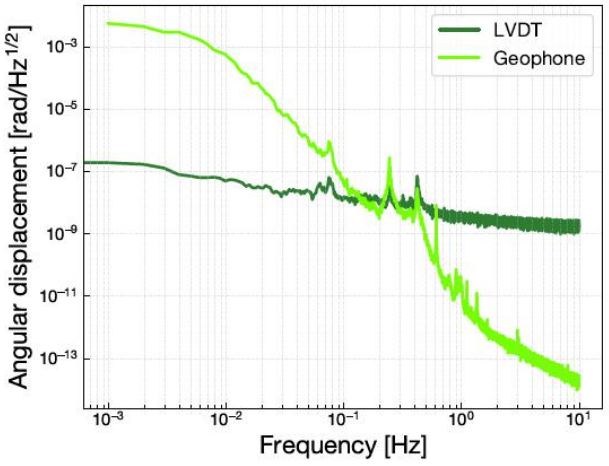

(c) Yaw

by K. Okutomi

Measured horizontal displacements of IP reach 10^{-11} m/Hz$^{1/2}$ level at 1Hz.

Direct measurement of DP motion

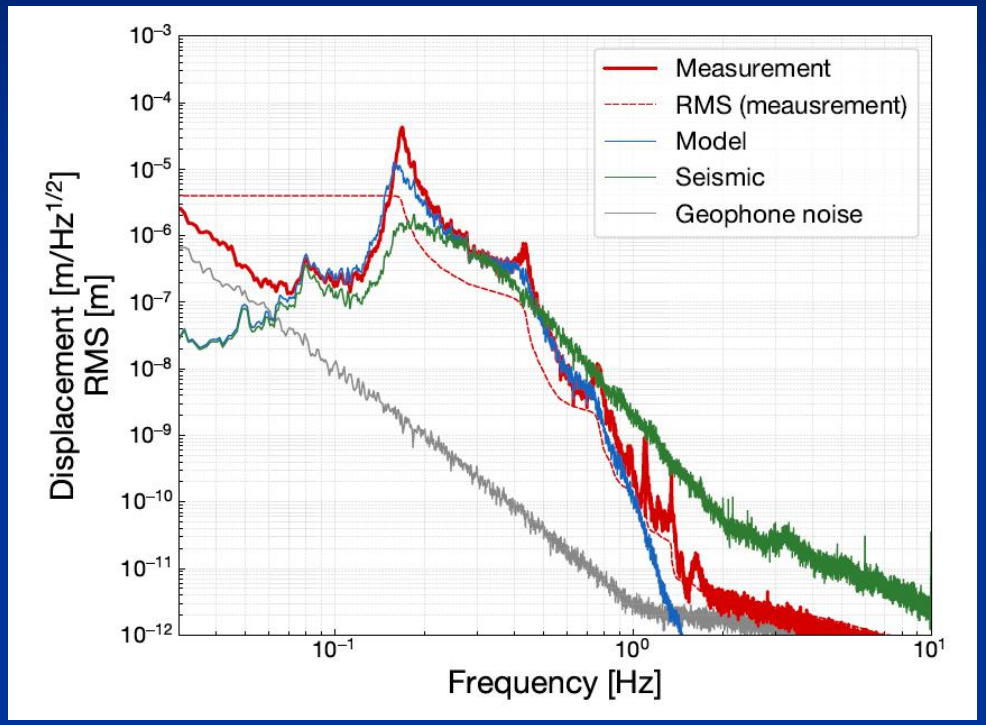

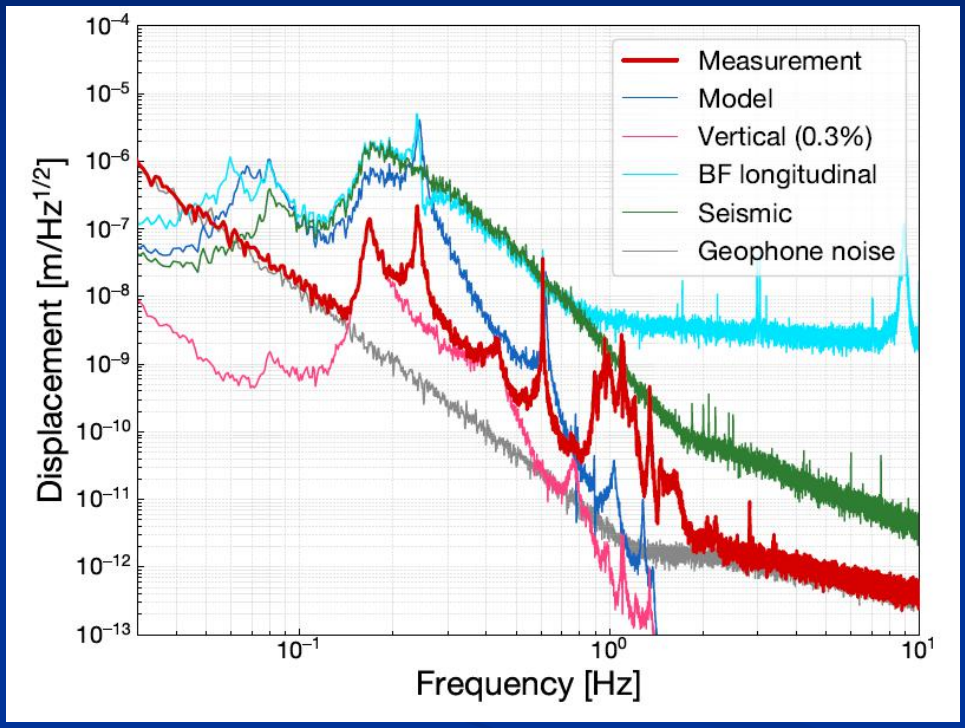

by K. Okutomi

Measured displacement of DP in vertical (left) and horizontal (right). Horizontal displacement at the frequency lower than 0.6Hz is too small. This is mystery.

Spectrum of X-arm fluctuation

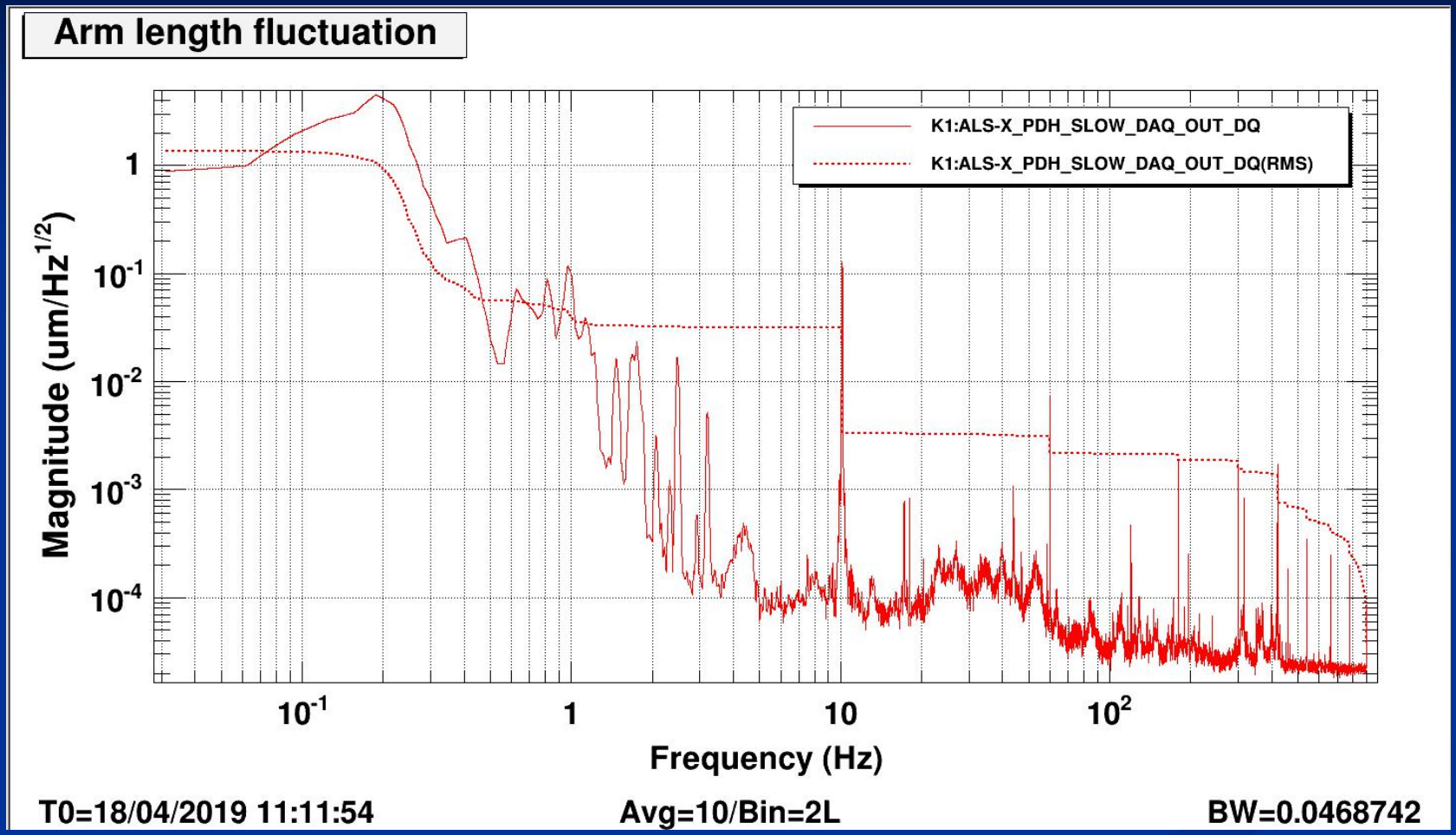

by Y. Enomoto

Spectrum of arm length fluctuation obtained in the first lock of X-arm.
The floor level is comparable with the noise level due to the frequency flucutation of light source.

Common mode rejection in Kamioka site

Poster #108: K. Miyo, Plan for the global control using strain-meter for KAGRA

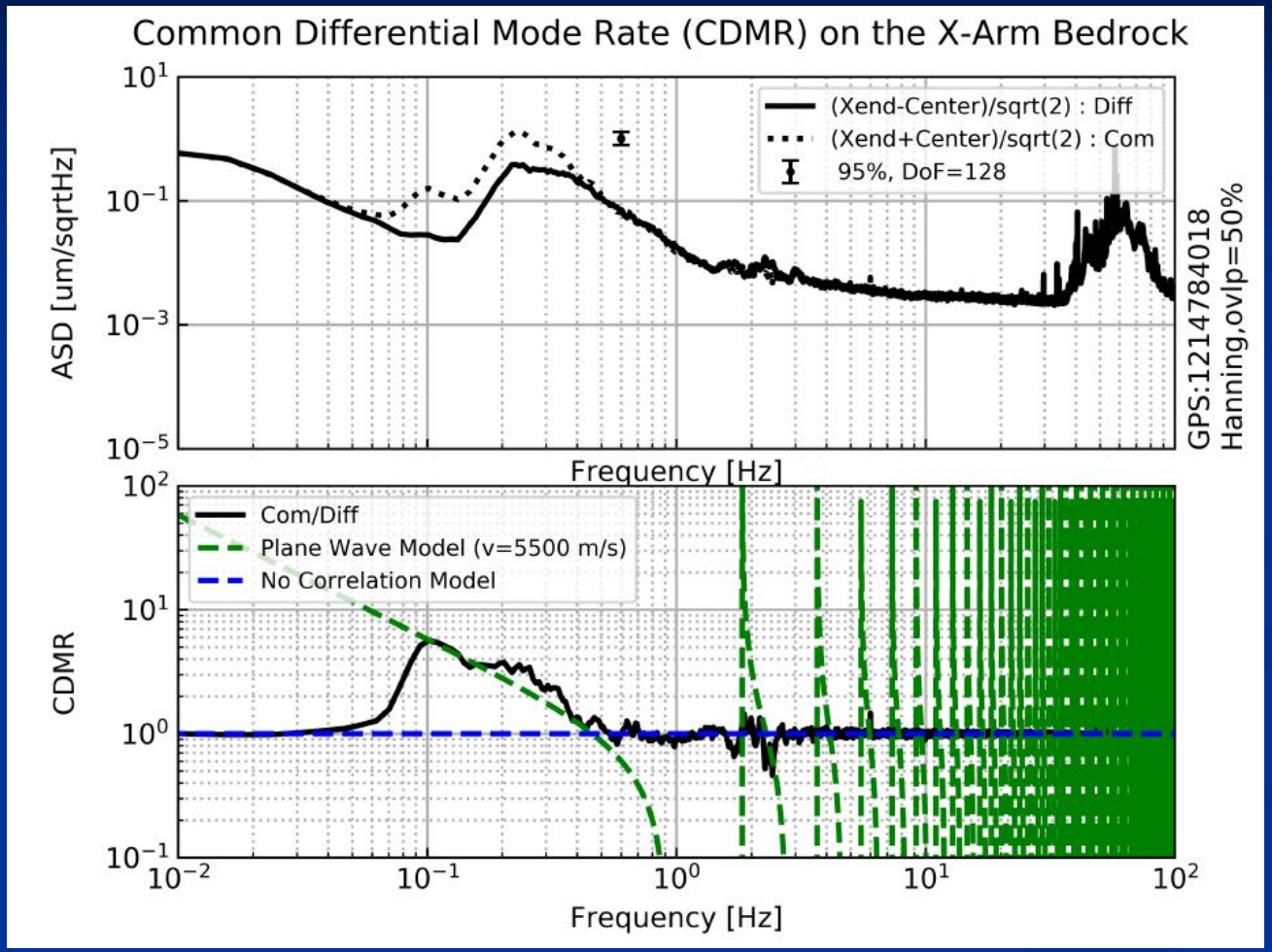

*The plane wave model is very naively calculated from velocity of P-wave measured in the CLIO site.

by K. Miyo

Spectrum of displacement measured by seismometers put in the center area and the X-end. Common mode rejection is effective around the microseisms due to the hard rock condition of Kamioka mine.

Summary

- Installation of vibration isolation system (Type-A/B/Bp/C) was finished by 2018. Commissioning is on going toward O3.
- Modal basis damping for the filter chain was implemented and tested.
- Inertial damping for the IP is under optimization.
- Behavire of TMs is still in consideration. Common mode rejection is expected.

Backup materials

Installation of Type-A tower

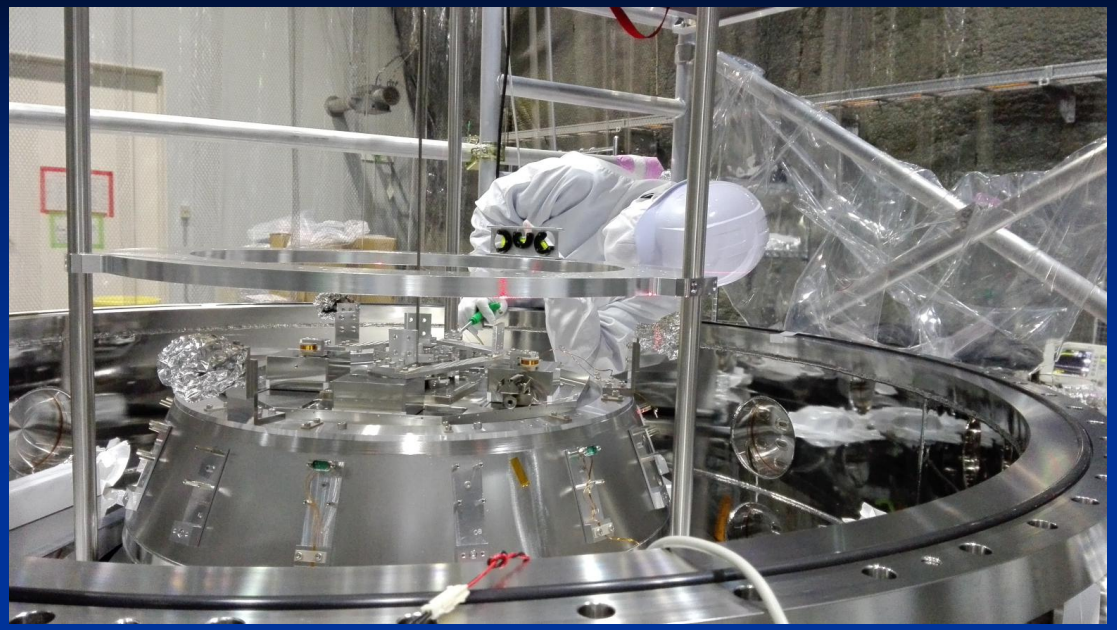

Adjustment of the BF and assemly of the BF damper.

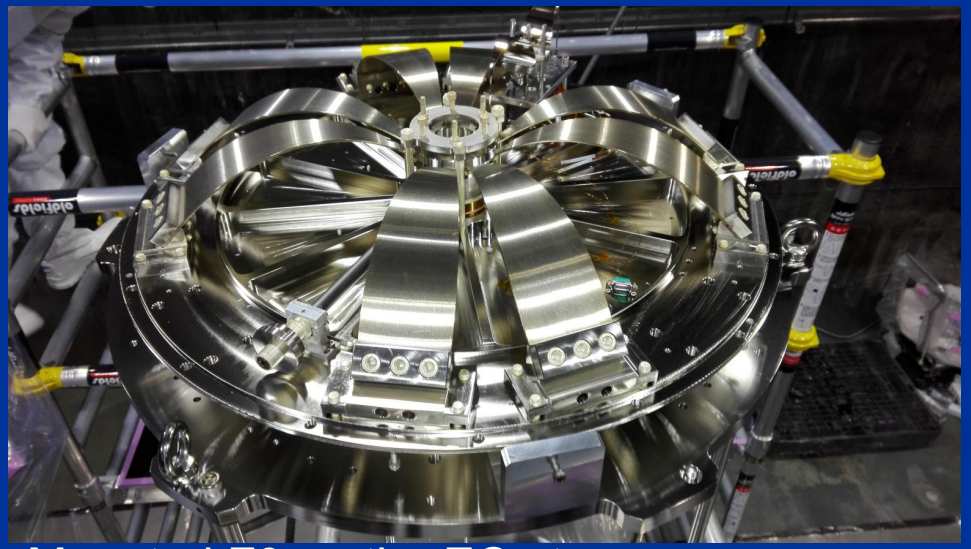

Mounted F3 on the EQ stop.

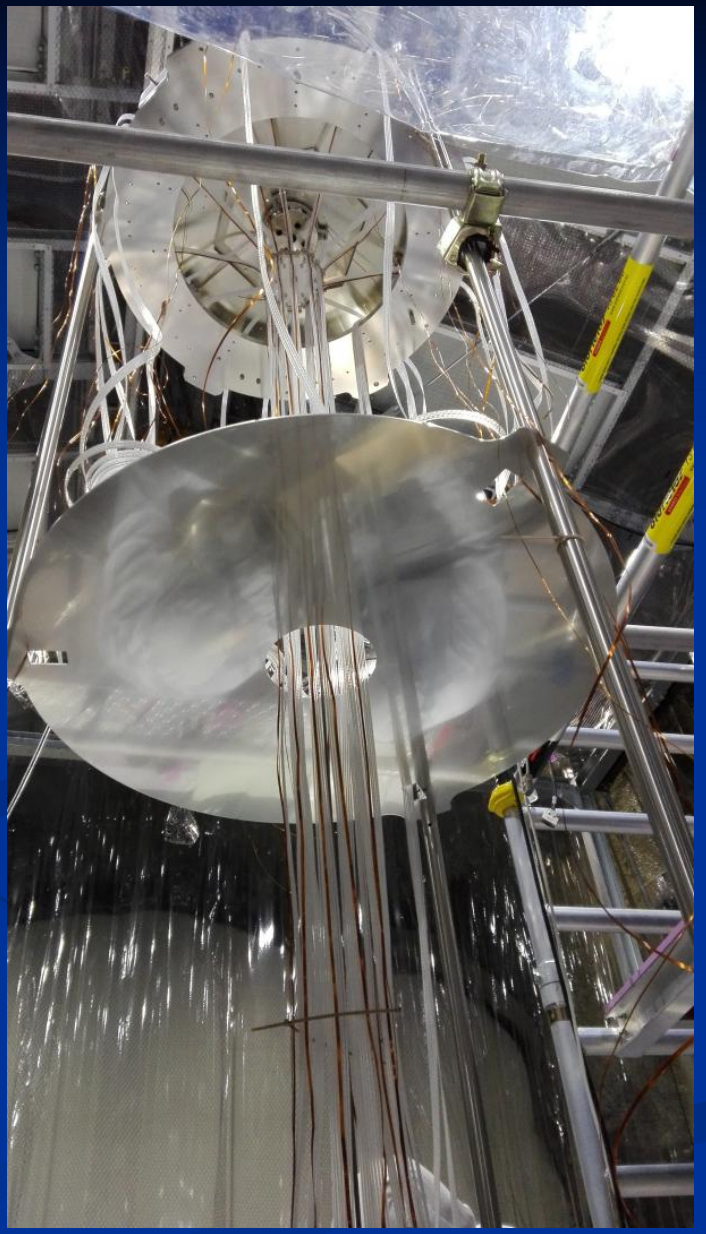

Cabling between the BF and the F3.

Installation of Type-A tower

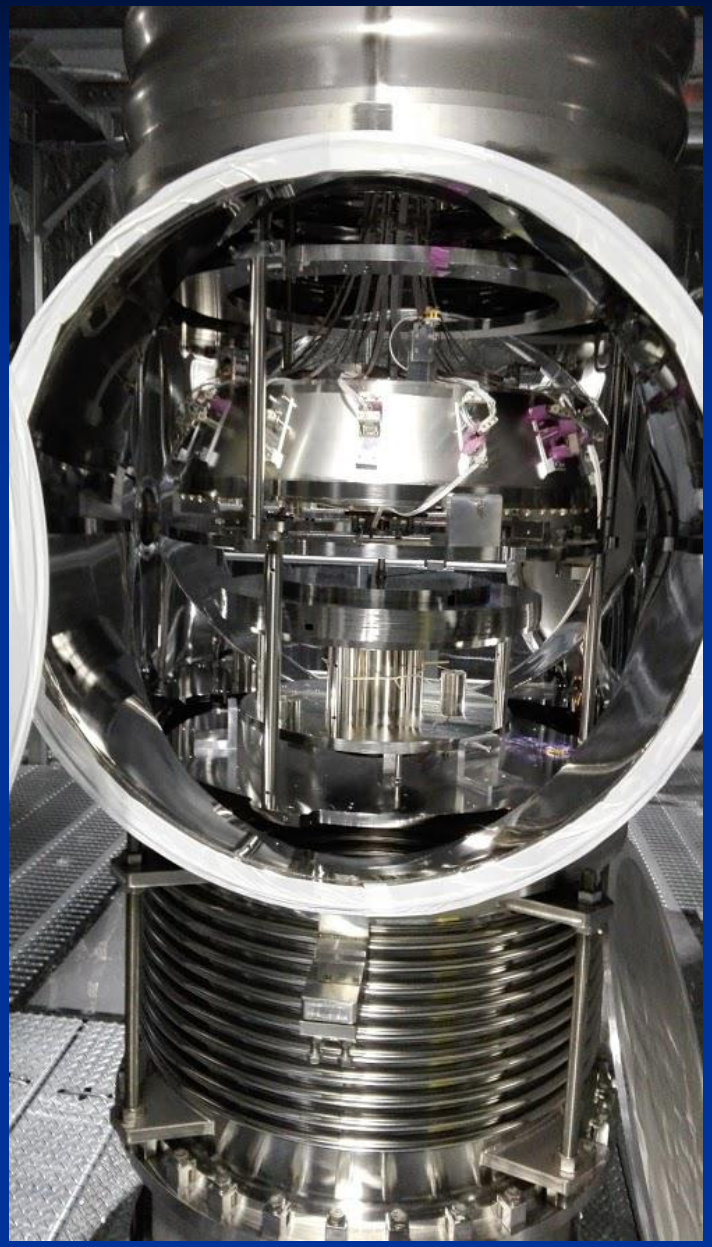

BF in the cross tube.

F1 with cables on the frame lock.

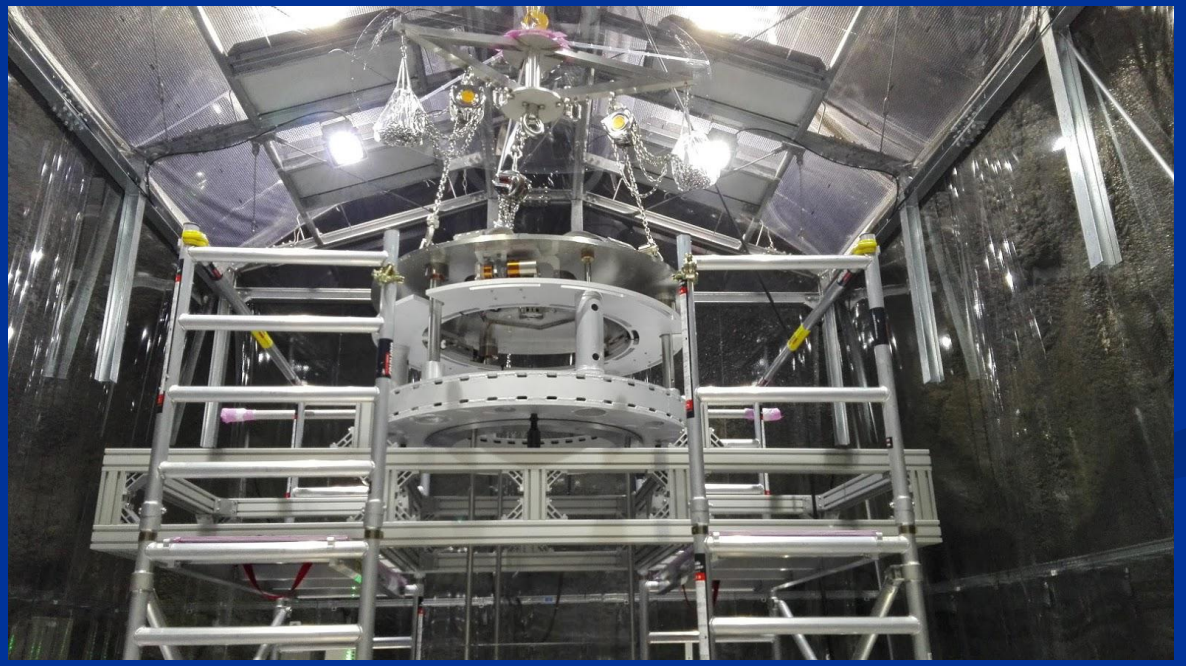

Pre-isolator on the bridge frame.

Sensor and actuator

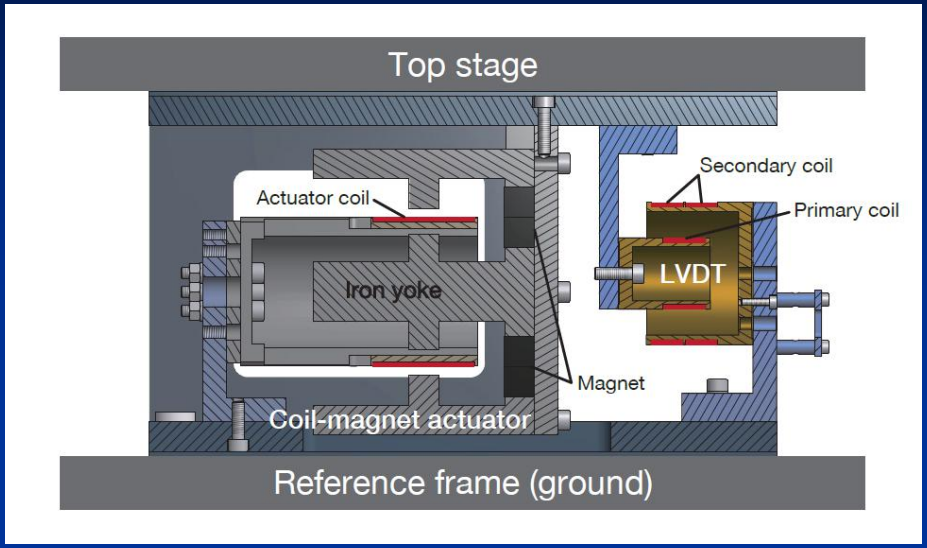

Horizontal LVDT-Actuator unit

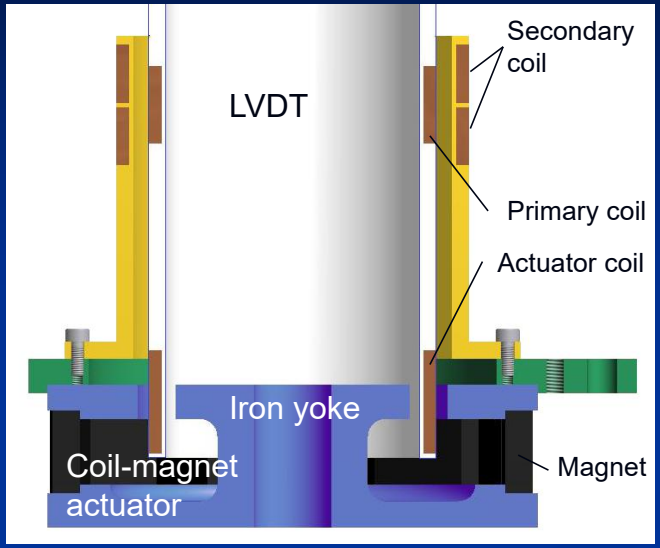

Vertical LVDT-Actuator unit

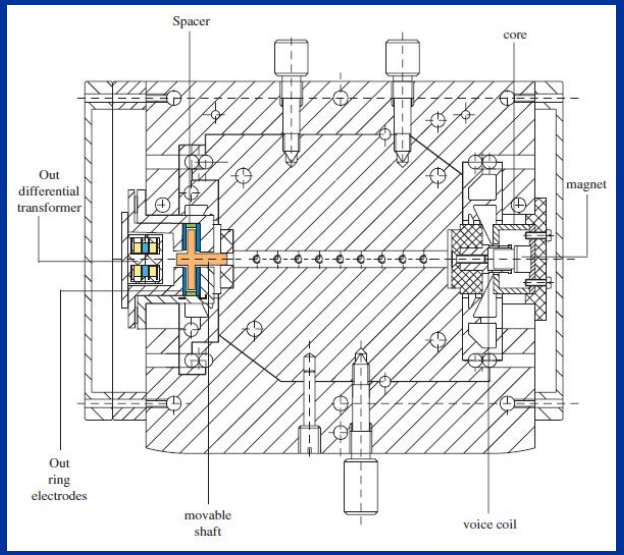

Inertial sensor (Accelerometer)

Inertial sensor (Geophone)

Torsion mode damping

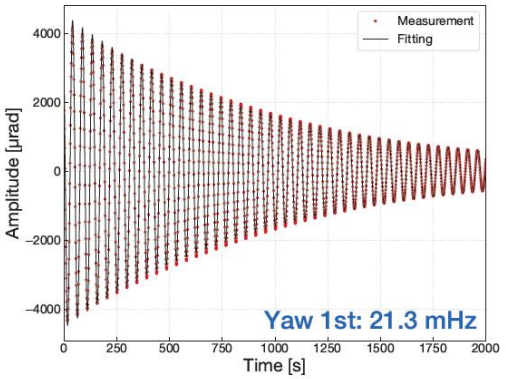

(a) 1st mode (undamped)

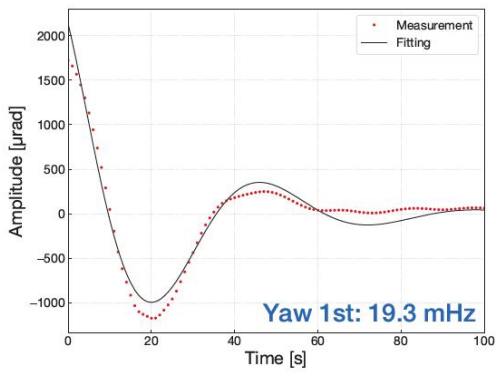

(b) 1st mode (damped)

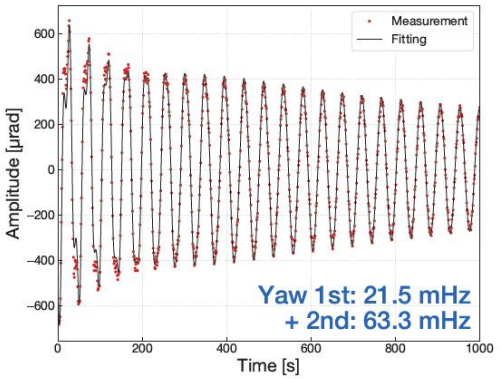

(c) 2nd mode (undamped)

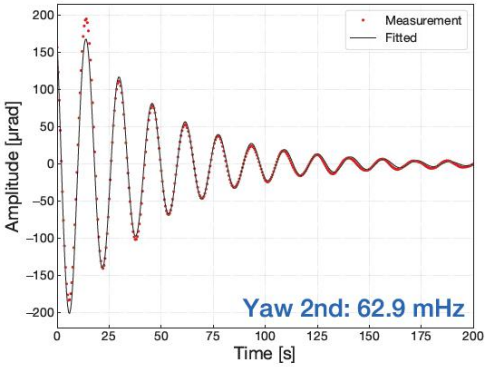

(d) 2nd mode (damped)

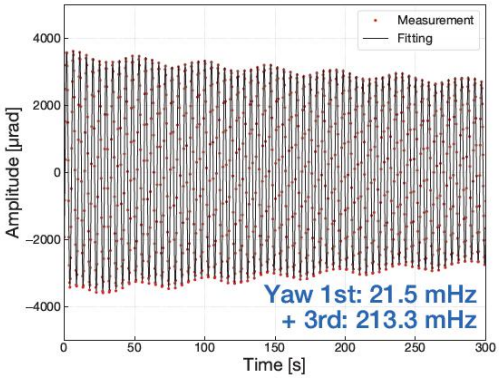

(e) 3rd mode (undamped)

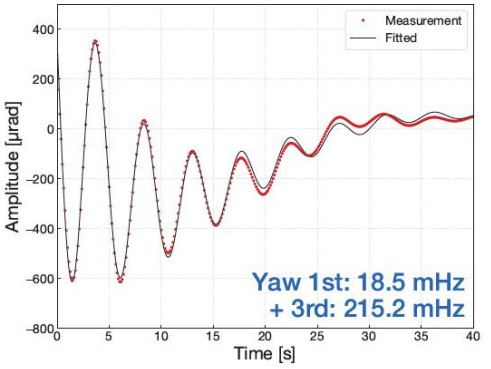

(f) 3rd mode (damped)

Spectrum of Michelson interferometer

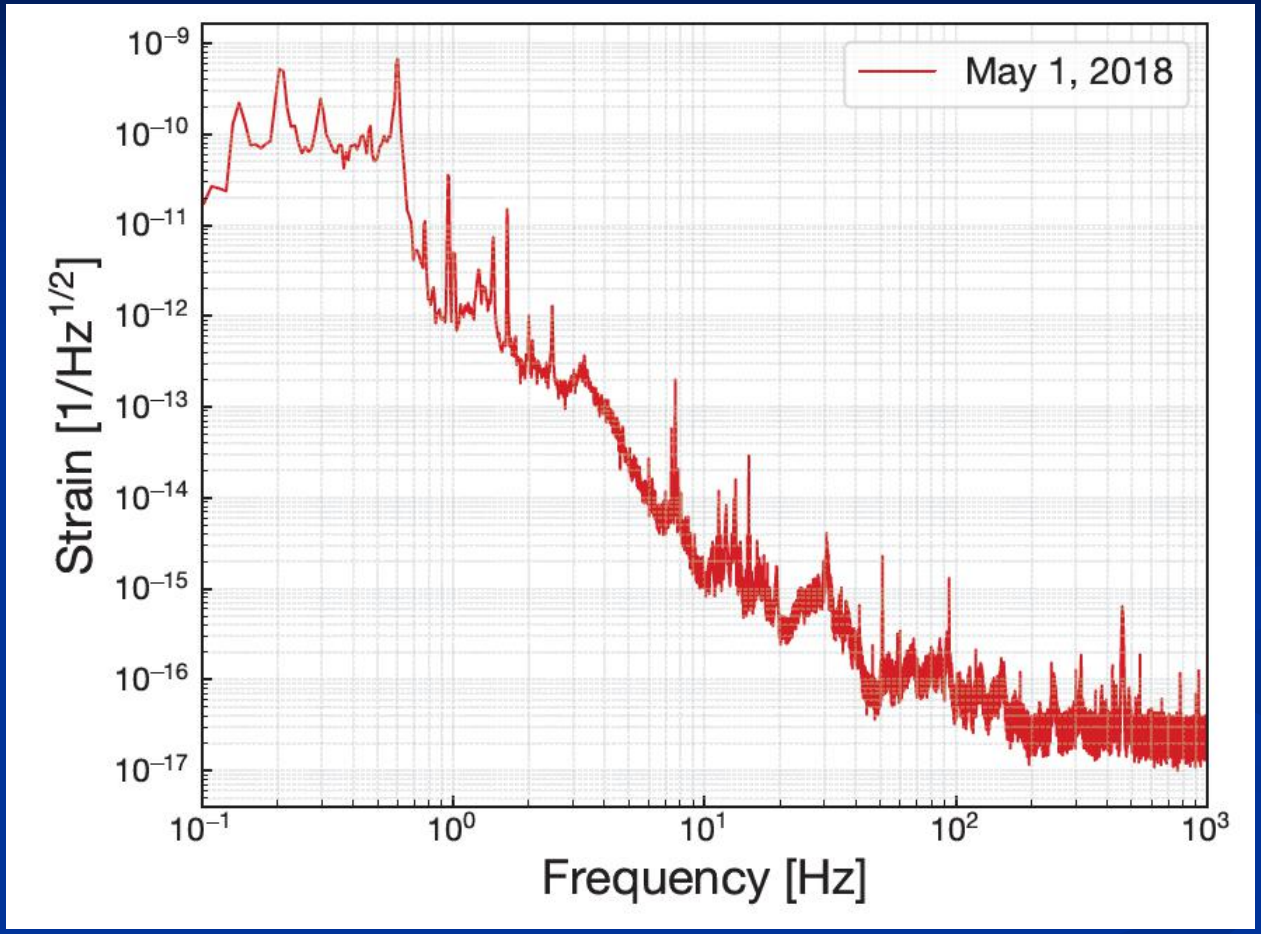

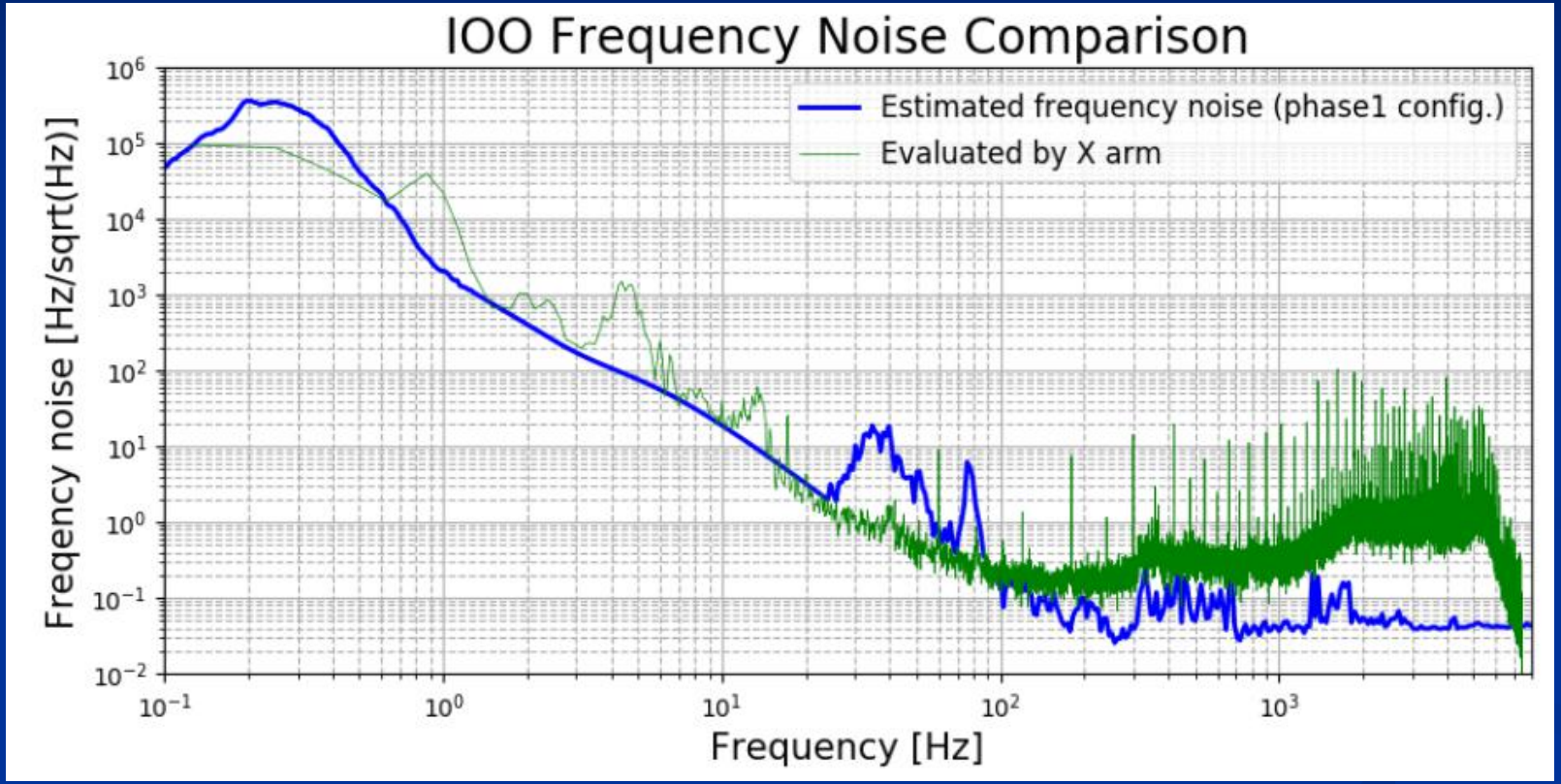
IOO Frequency Noise Comparison
Estimated frequency noise (phase1 config.)
Evaluated by X arm
Freqency noise [Hz/sqrt(Hz)]
Frequency [Hz]
10^{6}
10^{5}
10^{4}
10^{3}
10^{2}
10^{1}
10^{0}
10^{-1}
10^{-2}
10^{-1}
10^{0}
10^{1}
10^{2}
10^{3}